AGU PUBLICATIONS

JGR

Journal of Geophysical Research: Oceans

RESEARCH ARTICLE

10.1002/2016JC011688

Key Points:
- The waters off Morocco are under the influence of multiple natural and anthropogenic Cd sources
- Cd distributions from 22°N to 30°N are predominantly controlled by upwelling and phytoplankton uptake
- The fractionation between Cd and P results from phytoplankton uptake and remineralization

Supporting Information:
- Supporting Information S1

Correspondence to:
M. Waeles,
waeles@univ-brest.fr

Citation:
Waeles, M., H. Planquette, I. Afandi, N. Delebecque, F. Bouthir, A. Donval, R. U. Shelley, P.-A. Auger, R. D. Riso, and L. Tito de Morais (2016), Cadmium in the waters off South Morocco: Nature of particles hosting Cd and insights into the mechanisms fractionating Cd from phosphate, *J. Geophys. Res. Oceans*, *121*, 3106–3120, doi:10.1002/2016JC011688.

Received 30 JAN 2016
Accepted 11 APR 2016
Accepted article online 15 APR 2016
Published online 13 MAY 2016

Cadmium in the waters off South Morocco: Nature of particles hosting Cd and insights into the mechanisms fractionating Cd from phosphate

Matthieu Waeles[1], Hélène Planquette[1], Imane Afandi[2], Nina Delebecque[1], Fatimazohra Bouthir[2], Anne Donval[1], Rachel U. Shelley[1], Pierre-Amaël Auger[3,4], Ricardo D. Riso[1], and Luis Tito de Morais[4]

[1]Université de Bretagne Occidentale, LEMAR UMR-CNRS 6539, IUEM, France, [2]Institut National de Recherche Halieutique, Casablanca, Plouzané, Morocco, [3]Instituto Milenio de Oceanografia and Escuela de Ciencias del Mar, Pontificia Universidad Catolica de Valparaiso, Valparaiso, Chile, [4]Institut de Recherche pour le Développement, UMR LEMAR 195, Plouzané, France

Abstract In this study, we report the distributions of total dissolvable cadmium and particulate cadmium from 27 stations in southern Moroccan coastal waters (22°N–30°N), which is part of the North-West African upwelling system. These distributions were predominantly controlled by upwelling of the North Atlantic Central Waters (NACWs) and uptake by primary production. Atmospheric inputs and phosphogypsum slurry inputs from the phosphate industry at Jorf Lasfar (33°N), recently estimated as an important source of dissolved cadmium (240 t Cd yr^{-1}), are at best of minor importance for the studied waters. Our study provides new insights into the mechanisms fractionating cadmium from phosphate. In the upper 30 m, the anomalies observed in terms of Cd:P ratios in both the particulate and total dissolvable fractions were related to an overall preferential uptake of phosphate. We show that the type of phytoplanktonic assemblage (diatoms versus dinoflagellates) is also a determinant of the fractionation intensity. In subsurface waters (30–60 m), a clear preferential release of P (versus Cd) was observed indicating that remineralization in Oxygen Minimum Zones is a key process in sequestering Cd.

1. Introduction

The Canary Current System (CanCS) is one of the four major eastern boundary upwelling regions of the world [*Wang et al.*, 2015]. It supplies large amounts of macronutrient and micronutrient to the surface waters, inducing high primary production (up to 5 gC m^{-2} d^{-1} [*Arístegui et al.*, 2004]) and phytoplankton biomass (Chl *a* up to 10 mg m^{-3} [*Lathuilière et al.*, 2008]) that sustains important fisheries and the economies of neighboring countries [e.g., *Belhabib et al.*, 2015]. Among these nutrients, bioactive trace metals such as cadmium (Cd) can impact phytoplankton growth and community composition [e.g., *Price and Morel*, 1990; *Xu et al.*, 2008; *Baars et al.*, 2014], in turn affecting marine ecosystems.

In the ocean, Cd has a nutrient-type profile and is regenerated in a shallow cycle like major labile algal nutrients, nitrate (NO_3^-) and phosphate (PO_4^{3-}) [*Boyle et al.*, 1976]. However, there are divergences in the global oceanic Cd-phosphate (here referred as P for simplicity) relationship, with a pronounced break ("kink") in the slope at P $\sim$ 1.3 µmol L^{-1}, indicating a net preferential removal of Cd from surface waters [*Elderfield and Rickaby*, 2000]. Although not fully understood, this decoupling of Cd from the P cycle has received much attention because of its importance in the use of foraminiferal Cd as a paleoceanographic tracer of past primary production [*Boyle*, 1988]. Early on, it was hypothesized that the net preferential removal of Cd relative to P could ensue from a preferential accumulation of Cd in microplankton [*Sherrell*, 1989], and/or from a slightly deeper regeneration cycle for Cd [*Boyle*, 1988].

Many studies have thus focused on the comparative assimilation of P and Cd in phytoplankton from laboratory cultures or field studies. For example, different factors were found to influence the uptake of Cd relative to P such as the type of planktonic assemblages in the Equatorial Pacific Ocean [*Abe*, 2005], the planktonic physiological state and the ambient Cd and P concentrations [*Kudo et al.*, 1996], the CO_2 partial pressure [*Cullen et al.*, 1999], or the availability of trace metals such as Zn, Mn, or Fe [e.g., *Price and Morel*, 1990; *Sunda and Huntsman*, 2000; *Lane et al.*, 2008, 2009; *Gault-Ringold et al.*, 2012]. In the case of Zn, it has been

demonstrated that Cd can substitute for Zn in the enzyme, carbonic anyhydrase, if Zn availability is low [*Price and Morel*, 1990]. In the case of Fe, *Sunda and Huntsman* [2000] showed that Fe-limited diatoms have an elevated cellular Cd due to lower growth rates but constant Cd uptake, whereas *Lane et al*. [2008, 2009] found evidence of faster Cd uptake rates in Fe-limited cells. Some of these factors, which explain the regional specificity of the dissolved Cd:P ratio in the upper water column, were also proposed for controlling the Cd-P behavior on a global scale. For example, by comparing Fe-limited HNLC areas to Fe-replete areas *Cullen* [2006] proposed that the kink in the global Cd-P relationship could be a direct consequence of different fractionation in Fe-replete and Fe-deficient conditions. It has also been suggested that the high Cd:P uptake ratios in the Southern Ocean could have a significant impact on the global Cd distribution because these waters flow northward into the various oceanic basins at intermediate levels [*Frew and Hunter*, 1992]. Recent stable Cd isotope studies in the Southern Ocean [*Abouchami et al*., 2014; *Baars et al*., 2014] and the studies by *Yeats* [1998] and *Xie et al*. [2015] in the South Atlantic Ocean support this hypothesis.

In contrast, the decoupling of Cd-P during regeneration processes has received much less attention. The studies that have focused on such processes include studies of upwelling systems that have marked Oxygen Minimum Zones (OMZ) due to intense local mineralization, e.g., Arabian Sea [*Saager et al*., 1992], the Cape Basin [*Yeats et al*., 1995], or the Angola Basin [*Waeles et al*., 2013]. However, these studies also reported decoupled Cd and P profiles, with very low Cd:P ratios below the euphotic zone. In oxygen deficient areas of the North Atlantic Ocean, *Janssen et al*. [2014] recently showed that suspended particles have high Cd content and light Cd stable isotope ratios, suggesting the potential removal of Cd by coprecipitation with sulfides. Furthermore, distributions at intermediate levels in the South Atlantic Ocean [*Waeles et al*., 2013; *Xie et al*., 2015] indicate a decreasing Cd:P ratio from the subduction area at the Antarctic polar front toward the Northern Hemisphere, which suggests that (re)mineralization processes in oxygen deficient areas can have a major impact on the global Cd-P relationship.

There are few studies that have focused on the composition of Cd and P in particles specifically. *Knauer and Martin* [1981] and *Kuss and Kremling* [1999] reported Cd:P ratios in settling particles similar to that in the dissolved fraction in the northeast Pacific and northeast Atlantic oceans, respectively, while *Noriki et al*. [1999] argued that the differences in deep Cd:P ratios among ocean basins were probably due to differences in sinking particle composition ($CaCO_3$ in the North Atlantic versus opal in the North Pacific). This latter observation has recently been confirmed by *Quay et al*. [2015], who modeled the factors that control the interbasin variability of Cd/P of exported particles and the dissolved Cd/PO_4 in the surface layer and deep waters of the ocean, including the impacts of particle degradation and thermohaline circulation in the deep sea. Given that interactions between dissolved and suspended particulate species exert a control on the oceanic distribution of trace elements in seawater, simultaneously investigating the composition of suspended particles and the relationship with dissolved species should provide new insights on factors influencing Cd:P ratios. Among the myriad physical and biological processes, particles can sink downward to the deep ocean [*Buesseler et al*., 2007], can be resuspended from sediments [*Chase et al*., 2005], or horizontally mixed or advected [*Lam et al*., 2006], carrying trace elements along these pathways and generating gradients.

In coastal regions, Cd and P spatial distributions can be affected by physical and biological processes (including upwelling, biological assimilation, and particulate scavenging) and by external enrichments from atmospheric deposition or resuspension of continental margin sediments [e.g., *Delgadillo-Hinojosa et al*., 2001]. Off the coast of Morocco, a region influenced by upwelling, another potentially important source to consider is the direct release of phosphogypsum to coastal waters from the phosphate industry at Jorf Lasfar [*Gaudry et al*., 2007]. The recent modeling study of *Auger et al*. [2015] on the Cd uptake by plankton communities in the waters off Morocco indeed revealed a lower uptake of Cd from the natural source (upwelling) as compared to the uptake of Cd from the anthropogenic source (phosphogypsum). It is therefore important to investigate the distribution of Cd and P in shallow coastal environments in order to assess the influence of such anthropogenic sources which can equal or exceed natural inputs [e.g., *Wilhelmy and Flegal*, 1991], and to evaluate the relative importance of physical and biological processes in both dissolved and particulate compartments.

Here we report Cd and P data (total dissolvable and particulate concentrations) from 27 stations in Moroccan coastal waters (22°N–30°N) of the North-West African upwelling system. This study was conducted in summer which is the strongest period of upwelling events for this area [*Mittelstaedt*, 1991]. In this system, high primary production and intense remineralization is potentially influenced by anthropogenic inputs.

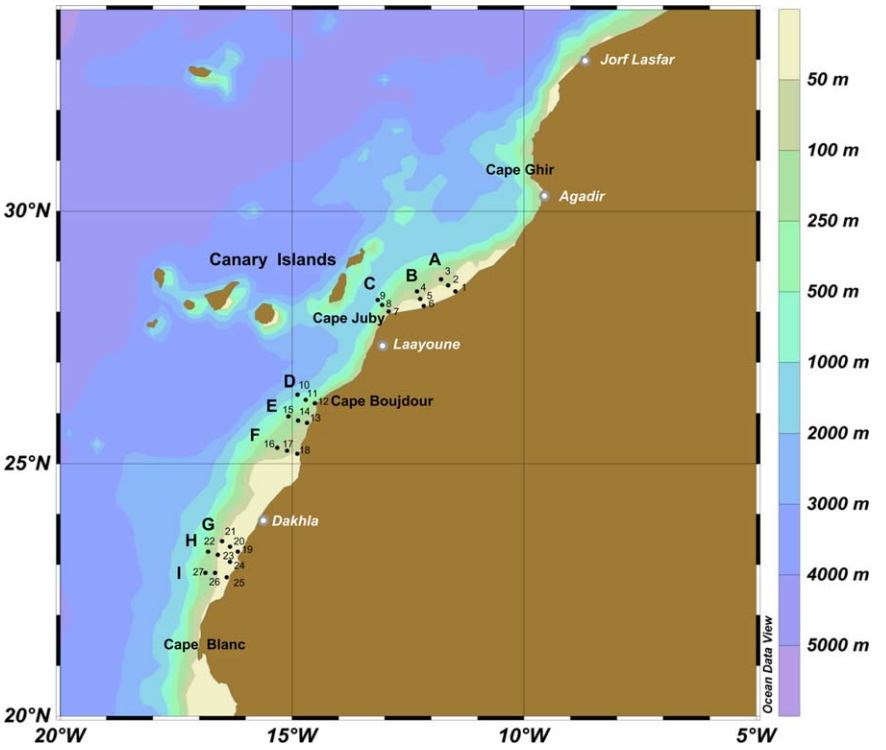

Figure 1. Map of stations (black dots and numbers) where total dissolvable and particulate samples were collected during the EPURE 2 cruise aboard the R/V Antea. Transect definitions are indicated by capital letters.

The aim of this study was to investigate the origin and nature of particulate Cd in the water column and to gain insights into the processes fractionating Cd from P in the global Ocean.

2. Material and Methods

2.1. Sampling and Filtration

During the EPURE cruise (11 July to 31 July 2013, R/V Antea), 27 hydrographic CTD stations were sampled for a suite of physical, biological, and chemical parameters using 8 L Niskin bottles. According to a test reported in *Riso et al.* [1994], no significant differences were observed for Cd concentrations between thoroughly rinsed Niskin and Go-Flo samplers. The bottles were mounted on a rosette equipped with a SBE 911+ Seabird CTD, two SBE43 dissolved oxygen sensors, an Aquatracka III fluorimeter, a Tritech sonar altimeter and a Sea Point optical backscatter sensor. The sampling track closely followed the African coast, incorporating different meanders of the Moroccan upwelling. In particular, three zones that contribute to the strength of the coastal upwelling, due to their bathymetric features, were targeted: north of Cape Juby, south of Cape Boujdour, and south of Dakhla (Figure 1). In each zone, three sections were performed (Figure 1) with a total of 110 and 70 samples being collected for the total dissolvable Cd (Cd) and particulate Cd (pCd) fractions, respectively. At each station, four to five depths were typically sampled, including surface and bottom depths, and depths corresponding to the oxygen minimum, the fluorescence maximum, and 5–10 m below the fluorescence maximum. Oxygen profiles were calibrated by on-board analysis of discrete water samples using the Winkler method [*Aminot and Kérouel*, 2004] with an accuracy of 5 μM.

2.1.1. Total Dissolvable Cadmium (Cd)

Immediately upon recovery of the rosette, aliquots of unfiltered seawater were collected into acid-cleaned 125 mL Nalgene HDPE bottles. Before collecting the sample, the bottles were first rinsed three times with seawater. Unfiltered seawater samples were collected in order to minimize contamination issues on board. Despite cadmium has a very low affinity for adsorption onto solid surfaces [*Oakley et al.*, 1981], it can be highly absorbed by phytoplankton. Therefore, the Cd data presented in this study likely include a fraction of particulate organic cadmium. This should be the case at a few stations, notably station 5, 15 m depth, where the pCd exceeded the Cd concentration and a high fluorescence level (7.7 mg m^{-3}) was observed.

Table 1. Recovery of Determined Cd Concentrations as Compared to Certified Values for Seawater CRM (CASS-4 and NASS-5, NRCC)[a]

Reference Material		Cd	P	Al	Pb
CASS-4	n = 8	96 ± 9%			
NASS-5	n = 8	94 ± 7%			
BCR-414	n = 3	119* ± 15%	108 ± 14%	111 ± 15%	81 ± 10%

[a]Recovery of determined Cd, P, Al, and Pb concentrations as compared to certified or indicative* values for plankton CRM (BCR-414).

However, the median particulate fraction represented only 13% of the total dissolvable component indicating that total dissolvable concentrations can be generally considered representative of dissolved concentrations.

2.1.2. Particulate Cadmium (pCd)

Upon recovery of the Niskin bottles, off-line filtration was performed. Seawater was collected in a 2 L acid-cleaned LDPE receiving bottle that was modified for direct filtration by inversion, with an air vent at the bottom and a custom fabricated filter holder adapter replacing the normal cap. Filter holders (Swinnex®, Millipore) mounted with Polysulfone (0.45 μm Pall/Gelman Supor®) filters were connected and filtration started within 2 h of collection. Filters were cleaned following the protocol of *Planquette and Sherrell* [2012] and mounted in a filter holder within a class 100 clean room at the home laboratory in order to minimize contamination. Loaded filter holders were then tripled bagged and sent to the ship before departure. A custom rack was built in order to support the inverted bottles, allowing them to be agitated gently periodically during filtration to prevent particle settling on the bottle walls. A vacuum was applied to the filter holders, and typically 500 mL to 2 L of seawater was filtered for pCd determination. Filter holders were then double bagged and kept frozen at −20°C until analysis at the home laboratory.

2.2. Analytical Procedures

2.2.1. Total Dissolvable Cadmium (Cd) Determination

Samples were first thawed at room temperature then acidified to ∼pH 2 with 100 μL of concentrated 11 *M* suprapur HCl (Merck) per 125 mL of sample. Cd measurements were carried out using stripping chronopotentiometry (SCP). In this procedure, which is detailed elsewhere [*Riso et al*., 1997], Cd is concentrated on a mercury film electrode (diam. 5 mm) by applying a potential of −1200 mV (versus Ag/AgCl, KCl 3 *M*) under stirring conditions (4130 rpm). Stripping consisted of the application of a 0.5 μA current. The analytical signal, corresponding to the stripping time of the analyte, was obtained from the area under the peaks in dt/dE versus E plots allowing the charging current to be effectively eliminated. Determination of Cd concentrations was made by spiking each sample three times with standards. The method displays detection limit, precision, and reproducibility of 10 p*M*, 4%, and 3%, respectively, using a deposition time of 15 min. For determining concentrations <25 p*M*, the deposition time was increased. The accuracy of the method was regularly checked during the 4 month period of analysis with certified reference seawater samples (CASS-4 and NASS-5, NRCC, Ottawa Canada, Table 1).

2.2.2. Particulate Cadmium (pCd) and Particulate Phosphorus (pP) Determination

Prior to use for sample digestions, 15 mL flat-bottom Teflon vials (Savillex®) were cleaned following the protocol of *Planquette and Sherrell* [2012]. Using empty-vial digestions, vials were tested individually for blanks and screened before use. Filters were transferred in these vials and digestion was performed using 1 mL of a solution of 8.0 *M* HNO_3 (Merck®-Ultrapur Grade) and 2.9 *M* HF (Merck®-Suprapur Grade) at 130°C. Solutions were then evaporated to near dryness on a hot plate within a Class 100 evaporation box (Alcoplast). Then, 300 μL of concentrated HNO_3 (Merck®-Ultrapur Grade) was added and the solution was again evaporated to near dryness. Following the dry down steps, residues were redissolved with 3 mL of 0.80 *M* HNO_3 (Merck®-Ultrapur Grade). This archive solution was then poured into precleaned 15 mL polypropylene tubes (Corning®) and archived until analysis on a high-resolution inductively coupled plasma mass spectrometry (HR-ICP-MS; ELEMENT 2, Thermo). Process blanks were digested using the same protocol.

For analysis, typically, 400 μL of the archive solution was added to 800 μL of 0.80 *M* HNO_3 (Merck®-Ultrapur Grade) spiked with 1 μg L^{-1} In into acid-washed 13 mm o.d. polypropylene centrifuge tubes with rounded bottoms (VWR). Samples were introduced to a PFA-ST nebulizer (Elemental Scientific Incorporated, Omaha, NE) via a modified SC-Fast introduction system consisting of an SC-2 autosampler, a six-port valve and a vacuum rinsing pump. Stock standard solution was prepared gravimetrically from primary standards (Cd, Al, and P), in 0.8 *M* HNO_3 (PlasmaCAL Calibration Standards). A six-point external standard curve was prepared

by serial dilutions and analyzed at the beginning, the middle, and the end of each run. Indium was added as an internal standard (~1 μg L^{-1}, as run in final solution) to all samples, standards, and blank solutions. Final concentrations of samples and procedural blanks were calculated from In-normalized data. Precision was assessed through replicate samples (every tenth sample was a replicate) and was better than 10% in all cases. Accuracy was determined from analysis of CRMs of plankton (BCR-414). Digest procedures were identical to those used for samples, except that BCR-414 powder was immersed in the acid, not refluxed. The mass of CRM digested was scaled to match acid/mass ratios used for suspended matter samples. Recoveries ranged from 108% (P) to 119% (Cd) and fall within the uncertainties of the reference material provided (Table 1). Finally, to ensure the Cd data were not biased by interferences, potential MoO^+ interferences were monitored during each run and a correction applied.

2.2.3. Nutrient and Pigment Determination

Samples were stored frozen at −80°C until determination of nutrients at the home laboratory with a Bran-Luebbe® A3AutoAnalyzer, with accuracies of 0.5 μmol L^{-1} for nitrate and 0.02 μmol L^{-1} for phosphate [*Oudot et al*., 1998]. For pigment determination, 500 mL seawater was filtered using 25 mm GF/F filters, which were stored frozen (−80°C) until analysis. Pigments were extracted at −20°C into 3 mL methanol with vitamin E acetate (Sigma Aldrich) as an internal standard. After 1 h, filters were disrupted using an ultrasonic probe for 10 s, and then the samples were refrozen at −20°C for one more hour. Extracts were centrifuged for 10 min (4°C, 3000 rpm), then filtered using 0.2 μm Acrodiscs filters. Analysis was performed on a complete Agilent technologies 1200 HPLC system with a Zorbax Eclipse XDB-C8 column (3 × 150 mm) and a diode array detector using the method of *Van Heukeelem and Thomas* [2001] modified by *Ras et al*. [2008]. Separation was based on a linear gradient established between a 70:30 methanol:28 m*M* tributyl ammonium acetate mixture and a 100% methanol solution. Pigments were identified by retention time and spectral matches with pigments standards obtained from DHI-Water and Environment, Denmark. Optical densities were monitored at 450 nm for most pigments, except chlorophyll *a* and derivatives which were detected at 667 nm. Pigment concentrations were calculated from the peak areas with an internal standard correction and with a response factor generated from calibration of the HPLC system using the DHI standards.

3. Results

3.1. Hydrography of the Study Area and Distributions of the Main Variables

The study area forms the eastern boundary of the North Atlantic subtropical gyre. Wind-driven upwelling off the coast of Morocco is strongest in summer and autumn north of 25°N, and is observed all year round (although it is more intense in summer) south of 25°N [*Mittelstaedt*, 1991]. The equatorward coastal jet arising from the geostrophic adjustment of the surface density gradient between cold upwelled coastal waters and the warmer open ocean waters [*Allen*, 1973] is particularly strong off southern Morocco [see *Auger et al*., 2015]. Upwelling-induced vertical motions generally occur within the 0–100 km coastal band, as estimated from the Rossby radius of deformation in the NW African region [*Chelton et al*., 1998], thus the coastal jet is confined to nearshore waters. The instability of upwelling fronts and coastal irregularities leads to the formation of filaments and eddies that enhance cross-shore exchanges [*Marchesiello et al*., 2003]. Upwelling filaments off Cape Ghir and Cape Boujdour are particularly responsible for strong seaward deflections of the coastal current [*Barton et al*., 1998]. Model-derived regional estimations of upwelling enrichment and residence time with Lagrangian particles by *Auger et al*. [2015] indicate maximum upwelling and minimum residence time off Cape Boujdour (sections D, E, and F), while residence time is maximum upstream of Cape Juby (sections A, B, and C) and in the South Sahara Bank close to the coast (sections G, H, and I), which may enhance primary production [*Lachkar and Gruber*, 2011].

The vertical distributions of temperature and salinity along the nine inshore-offshore sections (Figure 2) showed a variety of structures and upwelling intensities. Strong upwelling signatures were observed in the northern area with important negative temperature (T) and salinity (S) anomalies (~5°C and ~0.1, respectively) across the three sections (A, B, and C) of this area. In the central part (sections D, E and F), T and S negative anomalies were restricted to the coastal stations and strong horizontal gradients were observed with the occurrence of warm (>20°C) and salty waters (>36.6) offshore. The southern sections (G, H, and I) displayed much lower T and S variations and were essentially characterized by a thermal stratification at ~20 m depth. Indeed, the latter sections were performed during a relaxation event of coastal upwelling off

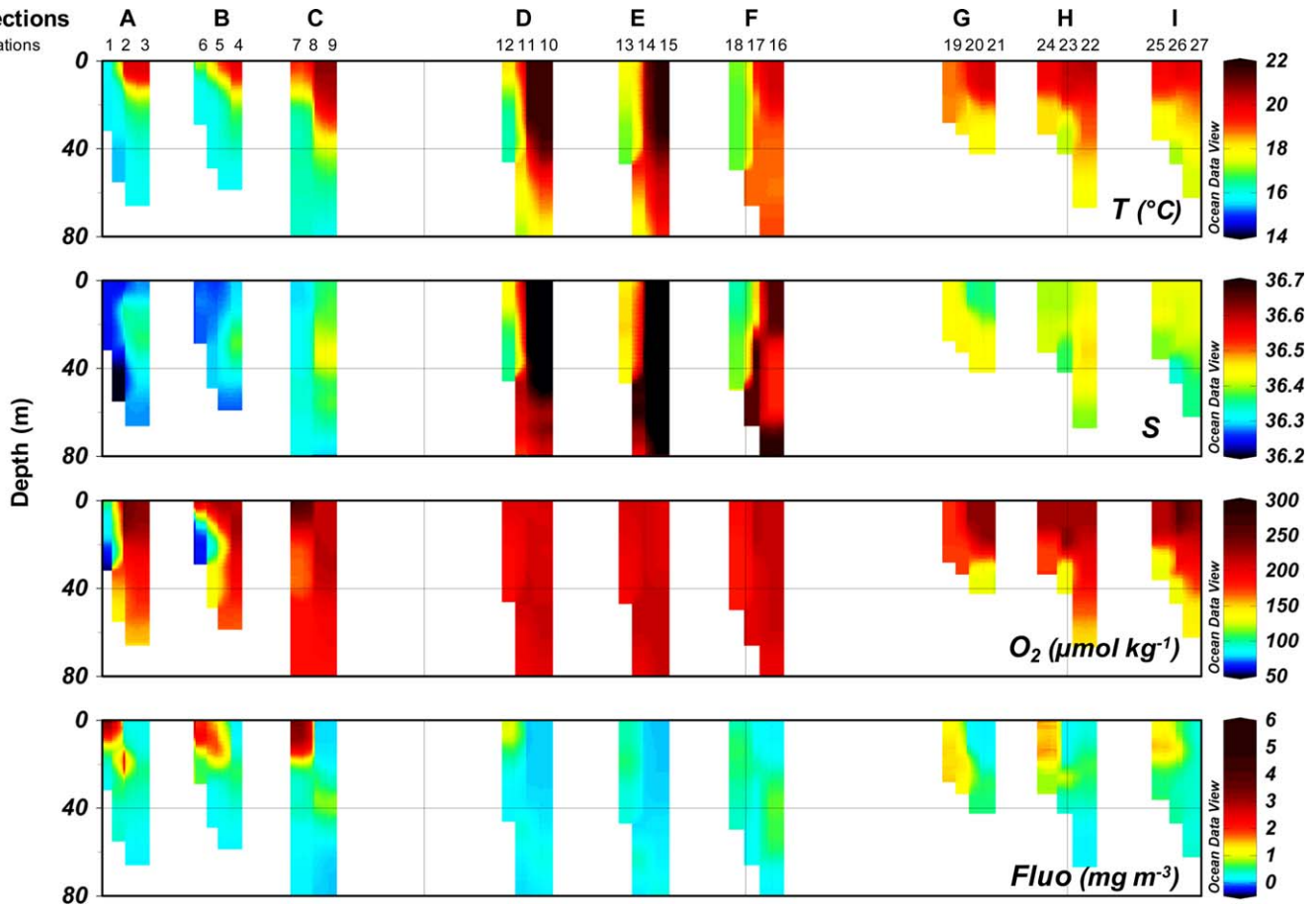

Figure 2. Vertical distributions of temperature (°C), salinity, dissolved oxygen (µmol kg^{-1}), and fluorescence (mg m^{-3}) along the nine sections (A to I). For each section, the inshore station is displayed on the left.

Morocco (see sea surface temperature data for July 2013, supporting information Figure S1). *T-S* diagrams for the various sections (Figure 3) show the occurrence of North Atlantic Central Water (NACW) in subsurface waters, in agreement with previous studies in this area [e.g., *Tomczak*, 1981; *Knoll et al*., 2002]. Moreover, NACW is essentially encountered with two types of superficial waters that will subsequently be referred to as SW1 and SW2, respectively: in the northern and southern areas, NACW was mainly encountered with SW1 (∼21°C, ∼36.3), whereas in the central area NACW was encountered with the warmer and saltier SW2 (∼22°C, ∼36.9). Due to the higher residence time in the southern and northern areas, SW1 may result from the mixing of SW2 with upwelling source waters within a wider coastal transition zone [*Barton et al*., 1998].

Fluorescence and dissolved oxygen distributions show strong primary production and respiration close to the shore in the northern area with fluorescence concentrations greater than 2 mg m^{-3} (and up to 5 mg m^{-3}) in the depth range 0–20 m, and O_2 values below 100 µmol kg^{-1} in the underlying waters (∼30 m), a result of strong upwelling and relatively long residence time. In the central area, biological activity was less intense, as reflected in the fluorescence concentrations that rarely exceeded 0.2 mg m^{-3}, while oxygen levels remained constant, around 200 µmol kg^{-1}. This may be the signature of the intense coastal jet off Cape Boujdour delaying primary production downstream over the Sahara Bank where residence time further increases. Although less intense than in the northern area, relatively high fluorescence (1.0–1.5 mg m^{-3}) and low oxygen (120–150 µmol kg^{-1}) patches were also observed in the southern area.

3.2. Cd and P Distributions

Total dissolvable (Cd) and particulate Cd (pCd) concentrations along the various sections are displayed in Figure 4. Overall, Cd is predominantly in the total dissolvable phase, with concentrations ranging from 40 to

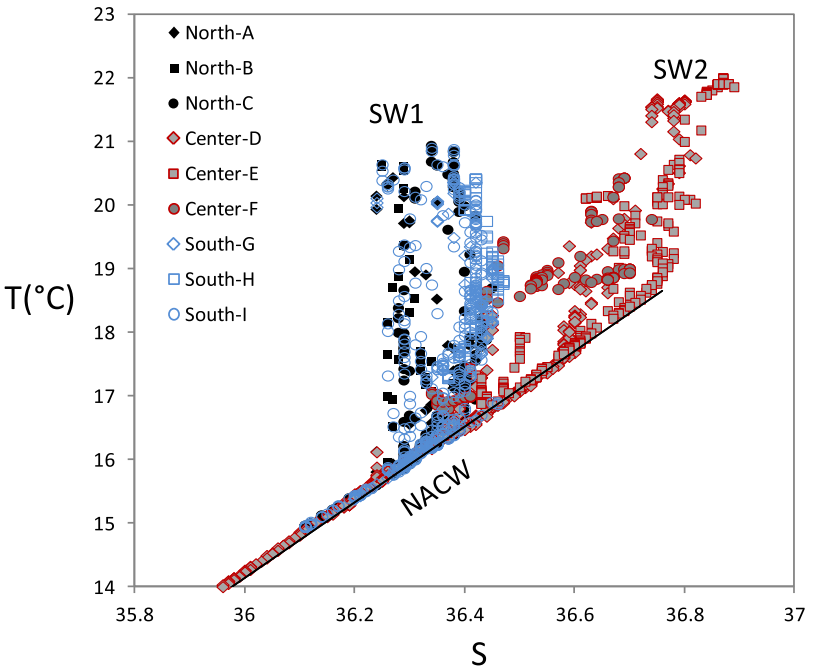

Figure 3. T-S diagrams at the various sections for the northern (black), central (red), and southern (blue) areas. The black line indicates the typical T-S relationship of the North Atlantic Central Waters [*Tomczak*, 1981; *Knoll et al.*, 2002]. SW1 and SW2 correspond to different superficial water types.

370 p*M* in the northern area and from 40 to 420 p*M* in the southern area. Lower values were measured in the central area, ranging between 10 and 210 p*M*. Particulate Cd (pCd) concentrations were significantly lower, ranging between 2 and 218 p*M* in the northern area, between 0.6 and 47 p*M* in the central area, and between 3 and 82 p*M* in the southern area.

For most sections, maximum Cd concentrations were encountered close to the coast and concentrations generally decreased offshore. This was particularly true for the northern sections, A and B, and the southern section, I, which displayed the strongest Cd horizontal gradients, with coastal stations being characterized

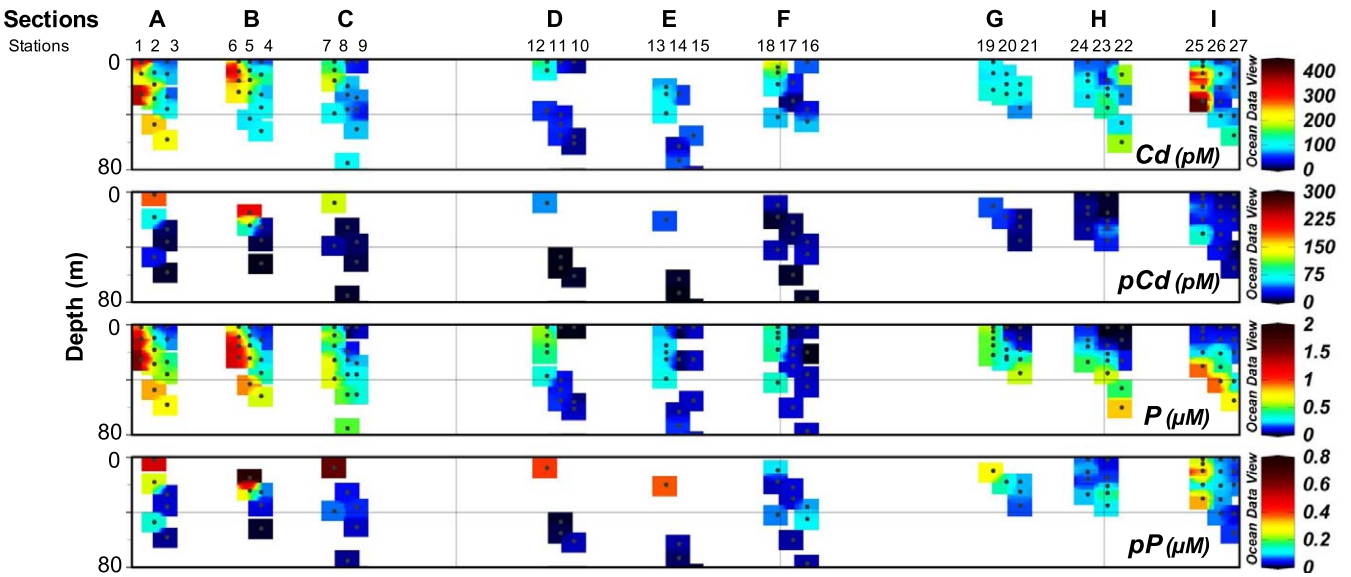

Figure 4. Vertical distributions of Cd (total dissolvable Cd, p*M*), pCd (particulate Cd, p*M*), P (Soluble Reactive Phosphorus, µ*M*), and pP (particulate P, µ*M*) along the nine sections (A to I). For each section, the inshore station is displayed on the left.

by values generally >200 p*M*. Vertical gradients of Cd were usually relatively low (with values below surface being generally in the range 50–120% of the surface values), but appeared more pronounced at offshore stations where increasing concentrations with depth were observed, in line with the expected nutrient-type distribution of Cd in oceanic waters [*Bruland and Lohan*, 2003].

The highest pCd concentrations, >200 p*M*, were only observed in the northern area close to the surface (0–20 m), and corresponded roughly to the areas of high fluorescence. In the southern area, at a station close to the shore (station 5, 30 m depth), pCd reached 82 p*M* just below the fluorescence maximum. Elsewhere, low pCd concentrations (<30 p*M*) were generally observed (i.e., for the central and southern areas, and for levels deeper than 30 m in the northern area). Overall, pCd concentrations tended to be higher in surface waters, which likely reflect the uptake of Cd by phytoplanktonic species in surface waters, followed by the sinking and subsequent decomposition of particulate matter.

At a first glance, similar trends to that of Cd were observed for P (Figure 4). Indeed, higher P levels were recorded for the productive northern (range: 0.02–1.50 μ*M*) and southern areas (0.02–0.93 μ*M*) as compared to the central area (range: 0.02–0.55 μ*M*). In the northern area, particularly at sections A and B where P concentrations decreased from values > 1.0 μ*M* at coastal stations to values < 0.6 μ*M* at offshore stations, strong horizontal gradients were observed. Although less marked, horizontal P gradients were also stronger than vertical gradients in the central area. In contrast, the southern area displayed stronger vertical gradients, with strongly P-depleted surface waters (P being generally < 0.2 μ*M* in the depth range 0–10 m).

Particulate P concentrations (pP) varied between 0.2 n*M* and 0.79 μ*M* with spatial distributions showing similar trends to pCd. The northern area was characterized by high pP concentrations in surface waters of the coastal stations, between 0.51 and 0.79 μ*M*. In the central area surface waters, pP ranged between 0.098 (section F) and 0.39 μ*M* (sections D and E). In the southern area, one should note the occurrence of relatively high pP concentrations (0.25–0.41 μ*M*) at coastal stations (sections I and G).

4. Discussion

4.1. On the Nature of the Particles Hosting Cd and Potential Influence of Anthropogenic Activities

Possible candidate sources of particulate cadmium in these coastal waters include inputs from the atmosphere, anthropogenic activities, sediment resuspension, or autochthonous biological production (dissolved Cd uptake or adsorption). In the following section, we examine each of the candidate pCd sources in the study area, discuss their relative importance, and use compositional data to estimate the particle types and host phases for Cd and associated elements.

4.1.1. Sediment Resuspension

Waves and tidal motion provide a mechanism for the resuspension of terrigenous, mineral particles to the upper water column in coastal waters [*Bale and Morris*, 1998]. Such a potential host phase for Cd in the sampled waters is unlikely as no pCd increase was observed in the deepest samples relative to the overlying depths (Figure 4). Moreover, Cd concentrations in the surficial sediment of this area were generally close to 0.2 μg g^{-1}, the background reference concentration defined by the OSPAR commission (http://www.ospar.org).

4.1.2. Mineral Aerosols

Although our study region underlies the main flow path of Saharan dust (~5°N–30°N, [*Prospero and Carlson*, 1972], measurements at Cape Spartel, northern Morocco [*Guieu et al*., 2010], and on the Canary Islands [*Gelado-Caballero et al*., 2012] concluded that aerosol Cd is primarily associated with fine particles (<1.0 μm), likely of anthropogenic origin. Indeed, *Gelado-Caballero et al*. [2012] argued that Cd and Pb in atmospheric deposition at Gran Canaria share a common, nonlocal, anthropogenic origin. This origin was ascribed to industrial emissions from the Atlantic coast of Morocco, northern Algeria, Eastern Algeria, and Tunisia [*Rodríguez González et al*., 2011]. Two lines of evidence that Saharan mineral dust is unlikely to be the predominant source of Cd during our survey are: (1) there was no direct evidence of deposition of Saharan mineral dust based on air mass back trajectory simulations (supporting information Figure S2), although we acknowledge there are some limitations to the use of air mass back trajectory simulations in this context (such as not being able to provide insight into entrainment of aerosols from the Saharan Air Layer) and (2) pCd and pAl were poorly correlated over the whole study area ($R^2 = 0.09$, $p = 0.01$, Figure 5a), given that Al is a frequently used tracer of mineral dust, the absence of a relationship between pCd and pAl reported

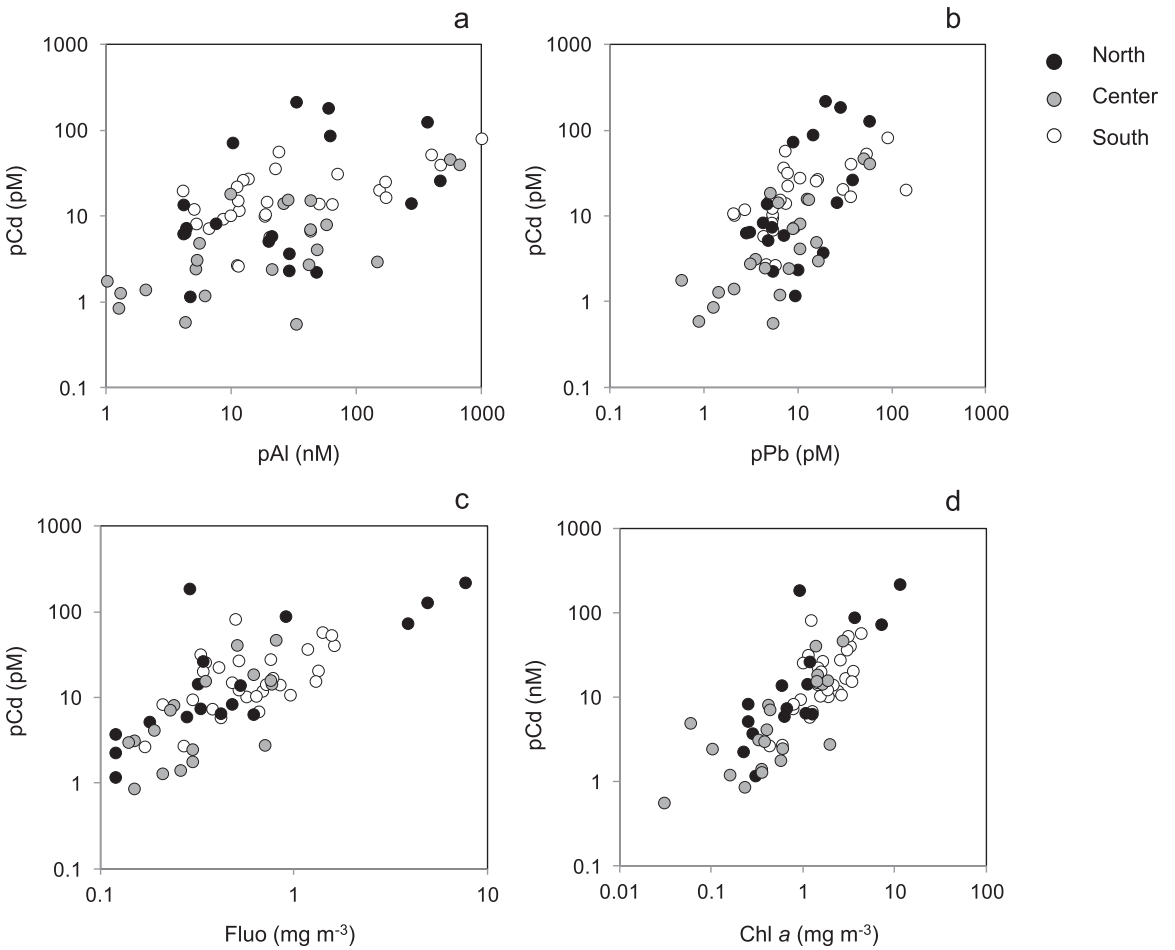

Figure 5. (a) pCd (p*M*) over pAl (n*M*), (b) pCd (p*M*) over pPb (p*M*), (c) pCd (p*M*) over fluorescence (mg m^{-3}), and (d) pCd (p*M*) over Chl *a* (mg m^{-3}) in the studied system. Black, grey, and white circles indicate samples collected in the northern, central, and southern areas, respectively.

here suggests that the two elements have different sources. Furthermore, the pCd:pAl ratios for the surface samples (depths < 30 m), i.e., 6×10^{-6}–7.2×10^{-3}, was significantly higher than the same ratio in Saharan aerosols, estimated as $(1.7 \pm 0.5)\ 10^{-6}$ [*Guieu and Thomas*, 1996]. Again, there are caveats to this approach, namely the different solubilities of Cd and Al in seawater that hinder interpretation but, when taken in conjunction with the other lines of evidence discussed, lend support to our hypothesis.

4.1.3. Anthropogenic Aerosols

The hypothesis of an anthropogenic aerosol source for pCd in the coastal waters of Morocco can be tested using relationships with other pollution-derived elements, e.g., Pb. We found that pCd was poorly correlated with pPb ($R^2 = 0.12$, $p = 0.004$, Figure 5b) and that the pCd:pPb molar ratio in SPM, with surface values ranging from 0.71 to 8.3, was substantially higher than the ratio reported for aerosols at Gran Canaria (0.07–0.18) and Cape Spartel (range 0.02–0.13) thus questioning a dominant anthropogenic aerosol Cd input to the studied coastal waters. Again, care is needed in this aerosol-SPM comparison because of the different element solubilities. However, *Theodosi et al*. [2010] showed a higher solubility in seawater for Cd associated with aerosols (as compared to Pb) which must lead to lowering the Cd:Pb ratios of these particles when deposited to seawater.

Yet this hypothesis of an anthropogenic atmospheric source cannot be completely discounted as the studied waters are potentially under the influence of a more local source of anthropogenically derived Cd, related to phosphate mining operation at Boucraa (26.32°N, 12.85°W). Indeed, a ~100 km conveyor belt transports phosphate from Boucraa to Laayoune harbor (27.05°N, 13.41°W) at a rate of ~2000 t h^{-1}. Although no data are available for atmospheric emissions from the phosphate industry, spillage from the

belt drifting to the south is clearly visible from satellite imagery (supporting information Figure S3). Our recent aerosol measurements (data not published) at the coastal stations of Agadir (30.46°N, 9.67°W) Laayoune (27.10°N, 13.41°W) and Dakhla (23.78°N, 15.90°W) indicate similar atmospheric Cd concentrations (in the order of 0.46–24 nmol Cd m^{-3} air) and similar Cd:Pb and Cd:Al ratios (range 0.1–20 mol mol^{-1} and 2–60 μmol mol^{-1}, respectively) to those observed at Gran Canaria and Cape Spartel. This observation, combined with the large differences in the Cd:Pb and Cd:Al ratios of the water column particles and the aerosols, suggests that this source is not the dominant input source to the study area.

4.1.4. Water Column Sources (Direct Discharges of Phosphogypsum Versus Upwelling) and Biological Control of pCd

Phosphogypsum slurry inputs at Jorf Lasfar represents a Cd source of 240 t Cd yr^{-1} [*Auger et al*., 2015], equivalent to the global oceanic atmospheric loads of Cd [*Duce et al*., 1991]. This slurry source can be considered, for the coastal waters off Morocco as, (1) a potential direct source of particulate Cd or, (2) a potential indirect source of particulate Cd through biological assimilation of dissolved Cd. Because the rate of dissolution of phosphogypsum particles (size range 10–100 μm) is relatively fast (>50% h^{-1}) [*Bolan et al*., 1991], it is unlikely that such particles will not undergo dissolution over a distance of 500 km from the Jorf Lasfar area to our studied area. Thus, we propose that the observed pCd appears to be essentially biogenic, i.e., associated with living phytoplankton or phytoplankton detritus, and that the anthropogenic contribution, if any (see next section), is indirect. The association of pCd with biogenic particles was evidenced by the strong correlation between pCd and fluorescence ($R^2 = 0.56$, n = 69, $p < 10^{-12}$, Figure 5c) and between pCd and Chl *a* ($R^2 = 0.48$, n = 66, $p < 10^{-10}$, Figure 5d) over the whole study region. In addition, significant correlations were also observed within each area between these factors (*p* values for pCd-fluorescence relationships were $<10^{-3}$, $<10^{-3}$, and <0.02 for North, Center, and South, respectively; *p* values for pCd-Chl *a* relationships were $<2 \times 10^{-3}$, $<10^{-4}$, and <0.03 for North, Center, and South, respectively).

The potential influence of the anthropogenic source was tested by comparing our Cd:P ratios with that of the North Atlantic Central Waters (NACWs) reported by *Yeats et al*. [1995], i.e., 0.25 mmol mol^{-1}, and with that of the Jorf Lasfar phosphogypsum reported by *Gaudry et al*., [2007], i.e., 0.84 mmol mol^{-1}. Indeed, upwelling of NACW and dispersion of anthropogenic loads of phosphogypsum by the phosphate industry at Jorf Lasfar (33°N) represent the two main dissolved Cd sources for the studied waters [*Auger et al*., 2015]. Although the majority of our Cd:P data, with values of 0.21–0.33–0.51 mmol mol^{-1} (first quartile-median-third quartile), fell close to the NACW ratio, a significant part of the data (~20%) was also found at levels over 0.6 mmol mol^{-1}. However, claiming that only part of the studied system is anthropogenically influenced is challenging for two reasons. First, it is difficult to accurately estimate the dissolved Cd:P ratio in regions of low dissolved Cd and/or low phosphate concentrations [*Quay et al*., 2015]. Indeed ~90% of Cd:P data over 0.6 mmol mol^{-1} are related to phosphate concentrations below 0.15 μ*M*. Furthermore, Cd and P are not incorporated in the phytoplankton at the same ratio as the ratio of the dissolved fraction. Fractionation factors reported for the North Atlantic waters [*Quay et al*., 2015; *Wu and Roshan*, 2015] are generally in the range 0.5–1.0 meaning that P is generally used preferentially relative to Cd. This preferential P uptake will lead to an increase of the Cd:P ratio in the dissolved fraction, which will become more pronounced at low P concentrations.

It is also worth noting that Cd-P fractionation is dependent on the composition of the planktonic assemblage. Indeed, we demonstrate in the following section that the high Cd:P ratios observed in the southern and central areas can be attributed to the dominance of diatoms. Based on the Cd:P ratio, the influence of anthropogenic inputs is not apparent. Bearing in mind the Cd-P fractionation upon uptake, the pCd:pP data were also used to assess the potential influence of anthropogenic activities. With the first quartile, median, and third quartile values of 0.13, 0.17, and 0.24, respectively, most of the pCd:pP values fell below the NACW ratio and thus relatively far from the phosphogypsum ratio suggesting that the upwelling natural source (as opposed to the anthropogenic source) exerts the major control on Cd uptake by primary production for the studied area. Furthermore, our pCd:pP range, i.e., 0.05 to 0.36 mmol mol^{-1}, was consistent with the Cd:P ratios (Figure 6) reported for a wide variety of phytoplankton cells collected across the North Atlantic Ocean [*Twining et al*., 2015].

4.2. The Role of Assimilation and Regeneration Processes on Cd-P Fractionation

Figure 7 represents the vertical distribution of Cd* and pCd* for the various areas. These concentrations illustrate relative enrichments or depletion of Cd relative to P as compared to the 0.25 ratio of the NACW.

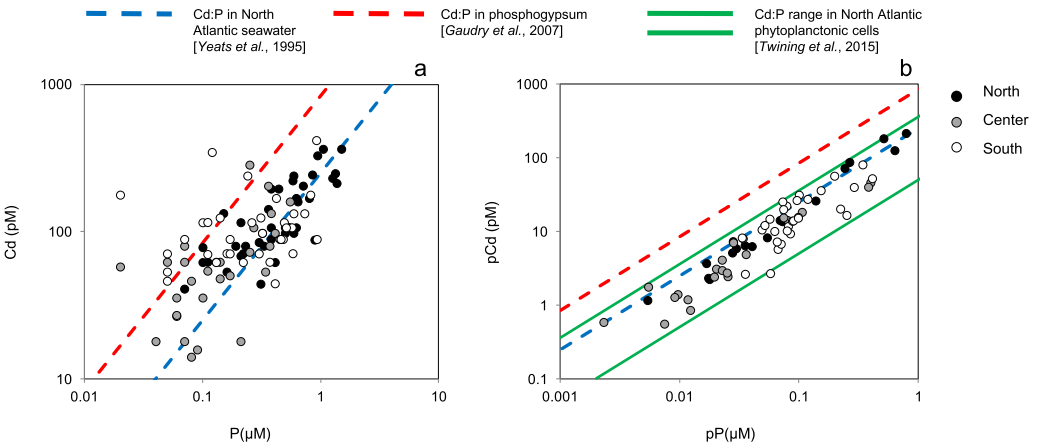

Figure 6. (a) Cd (p*M*) over P (μ*M*) and (b) pCd (p*M*) over pP (μ*M*) in the studied system. Black, grey, and white circles indicate samples collected in the northern, central, and southern areas, respectively. Blue dashed line indicates the Cd:P ratio reported in North Atlantic seawater [*Yeats et al.*, 1995]. Red dashed line indicates the Cd:P ratio in phosphogypsum [*Gaudry et al.*, 2007]. Green lines indicate the Cd: P range reported in phytoplankton cells of the North Atlantic [*Twining et al.*, 2015].

For the dissolved fraction, our data show a predominance of positive Cd* values close to the surface (0–20 m) whereas negative Cd* is generally observed between 20 and 60 m. Within the particulate fraction, an opposite relationship is observed with pCd* being predominantly negative above 20 m but close to 0 between 20 and 40 m. Interestingly, a geographical discrimination also appears in these distributions with lower Cd* and higher pCd* in the northern area (0–30 m depth layer).

The Cd* and pCd* were further examined by discriminating high fluorescence ($>$ 0.50 mg m^{-3}) and low oxygen ($<$200 μmol kg^{-1}) data. Positive Cd* and negative pCd* essentially corresponded to high fluorescence, showing an overall preferential assimilation by phytoplanktonic cells of P relative to Cd. This preferential assimilation of P is also illustrated by the fractionation factor (FF, with FF = (pCd:pP)/(Cd:P) [*Elderfield and Rickaby*, 2000]). FF values at high Chl *a* concentrations where indeed mostly found at values in the range 0.1–1.0 (Figure 7e). As these phytoplanktonic communities reside in a coastal setting with no known Fe or Zn limitation, passive adsorption by biogenic particles [*Tappin et al.*, 1993; *Dixon et al.*, 2006] is the likely process for the pCd pool enrichment, this process being less important than the active uptake of P.

The preferential assimilation of P, and the resulting low Cd:P ratio in particles, have also been hypothesized to be driven by the type of planktonic species [*Abe*, 2005]. During the cruise, the waters above 30 m of the whole studied area were generally dominated by microphytoplantonic species. Indeed, Figure 8a shows that this was particularly true for the northern and southern areas where the sum of fucoxanthin and peridinin, the two taxonomic pigments that are typical of diatoms and dinoflagellates respectively, in general contributed to the vast majority of the diagnostic pigments (defined by *Vidussi et al.* [2001] as the sum of: zeaxanthin + chlorophyll *b* + alloxanthin + 19′-hexanoyloxyfucoxanthin + 19′-butanoyloxyfucoxanthin + fucoxanthin + peridinin). If fucoxanthin was generally observed over the whole studied area, high levels of peridinin ($>$0.1 mg m^{-3}) were essentially observed in the northern area indicating a more important contribution of dinoflagellates in this area. This feature is illustrated in Figure 8b by the Peridinin:Fucoxanthin ratio which was significantly higher in the northern area as compared to the southern area ($p < 0.005$) and the central area ($p < 0.01$). The control of the pCd:pP ratio by the type of phytoplanktonic species is also shown in Figure 8c. In the northern area, where the contribution of dinoflagellates was more important, high pCd:pP ratios were indeed measured (mean: 0.26 mmol mol^{-1}, range: 0.19–0.36 mmol mol^{-1}). In the southern area, where diatoms dominated the planktonic pool, pCd:pP ratios were lower (mean: 0.16 mmol mol^{-1}, range: 0.05–0.29 mmol mol^{-1}). To our knowledge, this is the first time that such a control of the pCd:pP ratio is demonstrated from field observations. Noticeably, these results are in line with the reported ratios from culture experiments: 0.26 mmol mol^{-1} for dinoflagellates, 0.16 mmol mol^{-1} for diatoms $>$1500 μm^3 and 0.04 mmol mol^{-1} for diatoms $<$1500 μm^3 [*Finkel et al.*, 2007, and references therein]. Our data also suggest that the Cd:P ratio in the total dissolvable fraction, with higher ratios in the southern area than in the northern area (Figure 8d) could be the result, at least in part, from such a divergence in Cd-P assimilation.

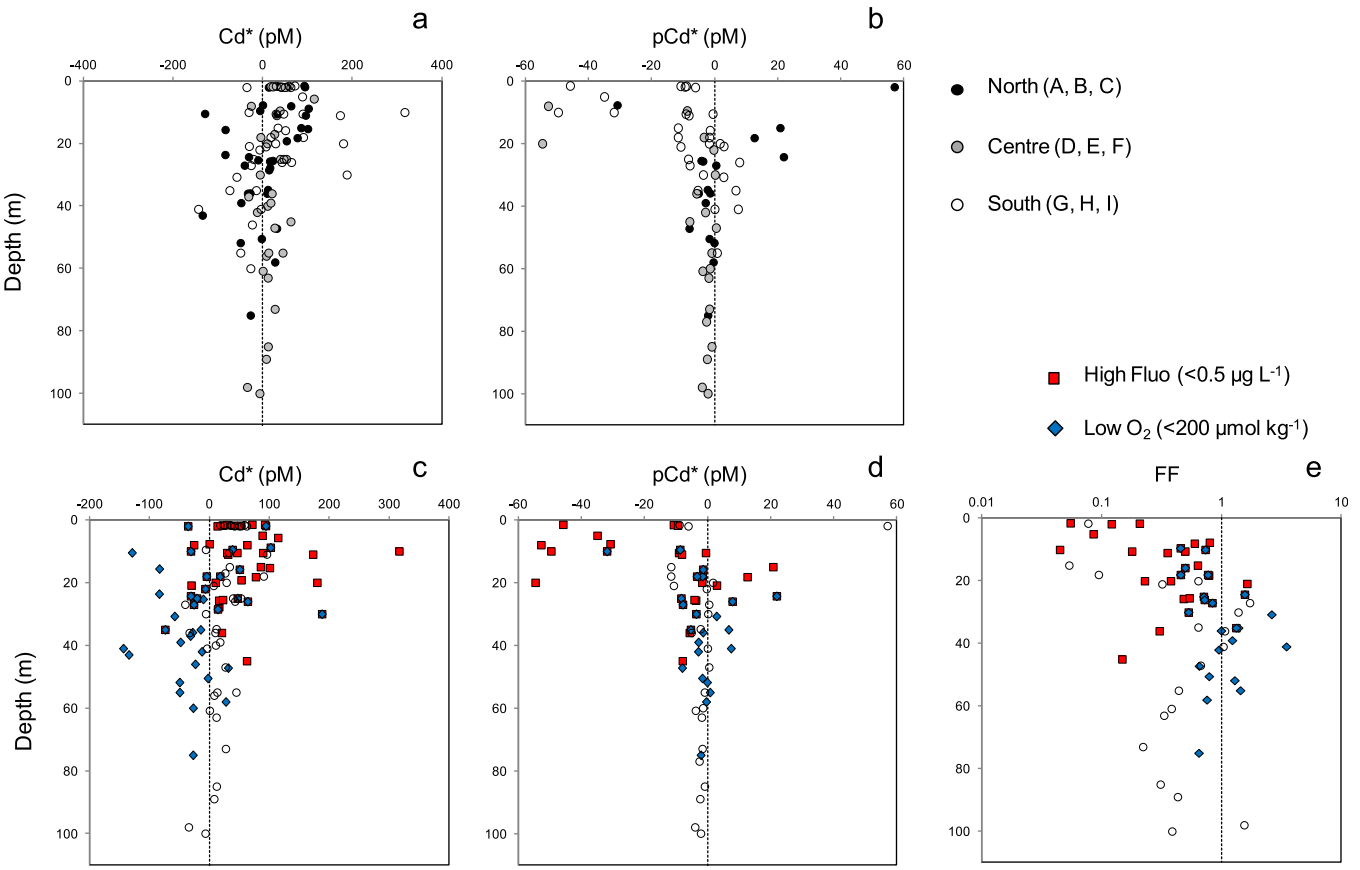

Figure 7. (top) vertical distribution of (a) Cd* and (b) pCd* for the northern (black circles), central (grey circles), and southern areas (white circles). Cd* is defined as $Cd^* = Cd_{measured} - 0.25 \times P_{measured}$, and pCd* as $pCd^* = pCd_{measured} - 0.25 \times pP_{measured}$, 0.25 being the Cd:P ratio of NACW [*Yeats et al.*, 1995]. (bottom) Vertical distribution of (c) Cd*, (d) pCd*, and (e) fractionation factor (FF) with FF = (pCd:pP)/(Cd:PO_4) [*Elderfield and Rickaby*, 2000] for fluorescence concentrations greater than 0.5 mg m^{-3} (red squares) and for low dissolved oxygen concentrations (<200 µmol kg^{-1}). White circles correspond to samples that did not fall into the conditions above mentioned.

The decrease of Cd* from surface waters to deeper, low-oxygenated waters (Figure 7a) indicates a preferential release of P relative to Cd through the microbial decay of organic matter. This is also corroborated by the observation that the FF generally increased with depth (Figure 7e). It is also worth noting that Cd* decreases toward overall negative values, and FF toward values > 1, which implies that this preferential release of P must exceed the preferential incorporation of P. This is an important result establishing that, almost independently of how P and Cd are assimilated, a net preferential removal of Cd will occur and that remineralization is also a key process for explaining the fractionation of Cd and P. Indeed, even in the southern area, where the highest preferential incorporation of P was observed in subsurface waters, negative Cd* values were found between 30 and 60 m depth. Very few hypotheses in relation to remineralization have been advanced to explain the decoupling of Cd and P in the global Ocean. Measurements in oxygen deficient zones [e.g., *Saager et al.*, 1992; *Waeles et al.*, 2013; *Janssen et al.*, 2014] strongly suggest that the preferential release of P could originate from the precipitation of CdS within the low-oxygenated environments of sinking aggregates. The present data from Moroccan coastal waters provide additional evidence for such fractionation.

5. Conclusion

Based on the elemental composition of suspended particulate matter, our study highlights the pervasive influence of biogenic particles on cadmium and phosphorus distributions in the study area. In terms of the distribution of dissolvable Cd and particulate Cd, upwelling of NACW was the predominant control. In contrast, atmospheric deposition and anthropogenic inputs of Cd did not have a dominant role in the sampling area covered by the EPURE cruise. However, it is worth noting that the dispersion of the phosphogypsum plume from Jorf Lasfar strongly depends upon the cross-shore transport lead by filaments at the major

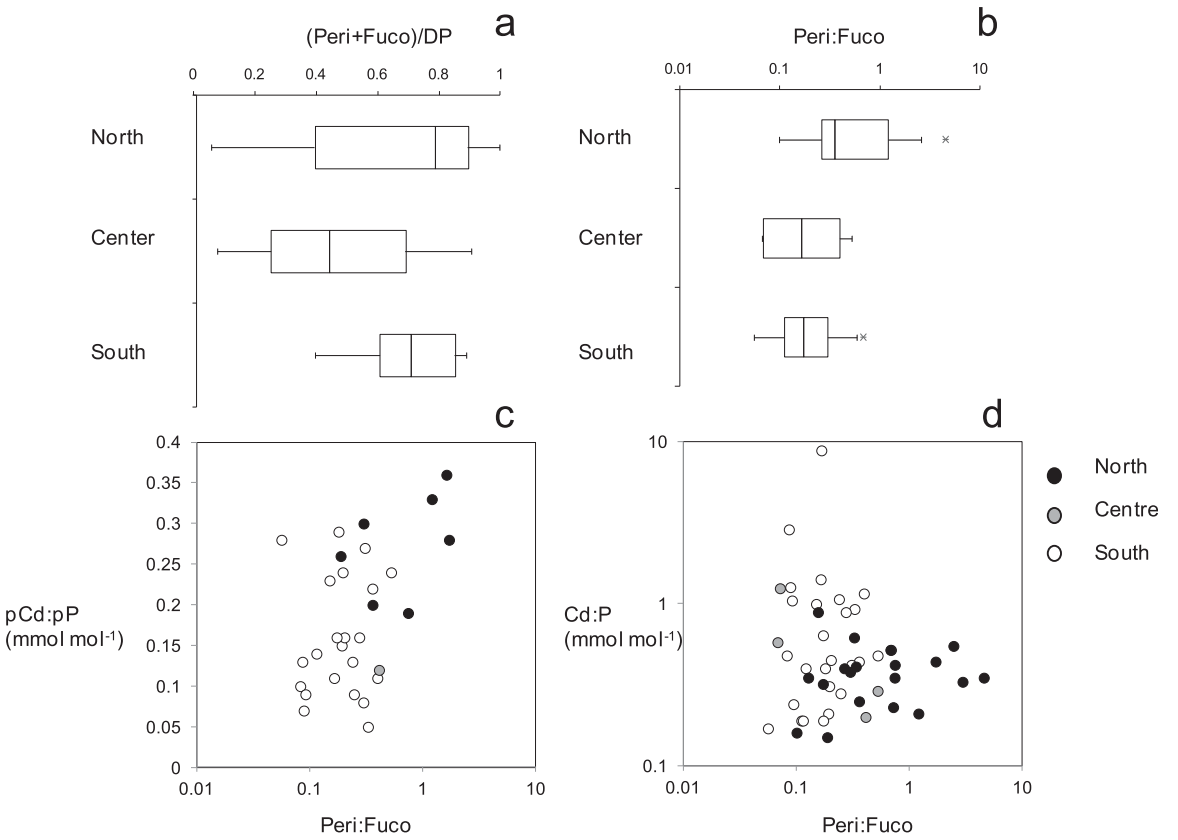

Figure 8. (a) Box plot representation of the (peridinin + fucoxanthin) over the various diagnostic pigments (DP, defined by *Vidussi et al.* [2001] as the sum of: zeaxanthin + chlorophyll *b* + alloxanthin + 19′-hexanoyloxyfucoxanthin + 19′ − butanoyloxyfucoxanthin + fucoxanthin + peridinin) for showing the importance of the microphytoplaktonic pool in the various areas; (b) box plot representation of the peridinin: fucoxanthin ratio for showing the dominance of dinoflagellates (high ratio) or diatoms (low ratio); (c) pCd:pP ratio (mmol mol^{-1}) over Peridinin:fucoxanthin ratio and (d) Cd:P ratio (mmol mol^{-1}) over Peridinin:fucoxanthin ratio for the northern (black circles), central (grey circles), and southern areas (white circles).

capes off Morocco (e.g., Cape Ghir) [*Auger et al.*, 2015]. Further investigation is needed closer to this slurry source to investigate how the biota is eventually affected. Our investigation on Cd and P in suspended particulate matter and seawater also highlights different fractionation processes. This fractionation appeared to be mainly driven by the type of phytoplanktonic assemblages in the upper 30 m, while a preferential release of P relative to Cd through the microbial decay of organic matter occurs at depth. This study is one of the few that have simultaneously investigated the distribution of dissolved and particulate cadmium and, as such, provides new insights into the biogeochemical cycling of Cd.

Acknowledgments

We are grateful to the helpful captain and crew of the R/V Antea and to the engineers of the Pole Spectrometry Ocean Brest (PSO, Brest, France) for their help in running ICP-MS measurements. Contour plots and profiles for Figures 1–3 and 5 were generated using Ocean Data View [*Schlitzer*, 2011]. This work was principally funded by ANR EPURE (P.I. L. Tito de Morais). Additional supports were provided by: ANR BITMAP (P.I. H. Planquette), LabexMER International (postdoctoral fellowship for R. Shelley), and Instituto Milenio de Oceanografia (ICM-Chile, writing phase for P. A. Auger). Supporting information provides data of this study (Table S1).

References

Abe, K. (2005), Apparent biological fractionation between Cd and PO 4 in the surface waters of the equatorial Pacific Ocean, *Mar. Chem.*, *96*(3), 347–358.

Abouchami, W., S. Galer, H. De Baar, R. Middag, D. Vance, Y. Zhao, M. Klunder, K. Mezger, H. Feldmann, and M. Andreae (2014), Biogeochemical cycling of cadmium isotopes in the Southern Ocean along the Zero Meridian, *Geochimica et Cosmochimica Acta*, *127*, 348–367.

Allen, J. S. (1973), Upwelling and coastal jets in a continuously stratified ocean, *J. Phys. Oceanogr.*, *3*(3), 245–257.

Aminot, A., and R. Kérouel (2004), *Hydrologie des Ecosystèmes Marins: Paramètres et Analyses*, Editions Ifremer, Plouzané, France.

Arístegui, J., E. D. Barton, P. Tett, M. F. Montero, M. García-Muñoz, G. Basterretxea, A.-S. Cussatlegras, A. Ojeda, and D. de Armas (2004), Variability in plankton community structure, metabolism, and vertical carbon fluxes along an upwelling filament (Cape Juby, NW Africa), *Prog. Oceanogr.*, *62*, 95–113.

Auger, P.-A., E. Machu, T. Gorgues, N. Grima, and M. Waeles (2015), Comparative study of potential transfer of natural and anthropogenic cadmium to plankton communities in the North-West African upwelling, *Sci. Total Environ.*, *505*, 870–888.

Baars, O., W. Abouchami, S. J. Galer, M. Boye, and P. L. Croot (2014), Dissolved cadmium in the Southern Ocean: Distribution, speciation, and relation to phosphate, *Limnol. Oceanogr.*, *59*, 385–399.

Bale, A. J., and A. W. Morris (1998), Organic carbon in suspended particulate material in the North Sea: Effect of mixing resuspended and background particles, *Cont. Shelf Res.*, *18*(11), 1333–1345.

Barton, E. D., J. Arıstegui, P. Tett, M. Cantón, J. Garcıa-Braun, S. Hernández-León, and K. Wild (1998), The transition zone of the Canary Current upwelling region, *Prog. Oceanogr.*, *41*(4), 455–504.

Belhabib, D., U. R. Sumaila, and D. Pauly (2015), Feeding the poor: Contribution of West African fisheries to employment and food security, *Ocean Coastal Manage.*, *111*, 72–81.
Bolan, N. S., J. K. Syers, and M. E. Sumner (1991), Dissolution of various sources of gypsum in aqueous solutions and in soil, *J. Sci. Food Agric.*, *57*(4), 527–541.
Boyle, E. A. (1988), Cadmium: Chemical tracer of deepwater paleoceanography, *Paleoceanography*, *3*(4), 471–489.
Boyle, E. A., F. Sclater, and J. M. Edmond (1976), On the marine geochemistry of cadmium, *Nature*, *263*, 42–44, doi:10.1038/263042a0.
Bruland, K., and M. Lohan (2003), Controls of trace metals in seawater, in *Treatise on Geochemistry, vol. 6, Marine Geochemistry*, edited by H. Elderfield, pp. 23–47, Elsevier, Oxford, U. K.
Bruland, K. W., J. R. Donat, and D. A. Hutchins (1991), Interactive influences of bioactive trace metals on biological production in oceanic waters, *Limnol. Oceanogr.*, *36*(8), 1555–1577.
Buesseler, K. O., et al. (2007), Revisiting carbon flux through the ocean's twilight zone, *Science*, *316*, 567–570, doi:10.1126/science.1137959
Chase, Z., B. Hales, T. Cowles, R. Schwartz, and A. van Geen (2005), Distribution and variability of iron input to Oregon coastal waters during the upwelling season, *J. Geophys. Res.*, *110*, C10S12, doi:10.1029/2004JC002590.
Chelton, D. B., R. A. Deszoeke, M. G. Schlax, K. El Naggar, and N. Siwertz (1998), Geographical variability of the first baroclinic Rossby radius of deformation, *J. Phys. Oceanogr.*, *28*(3), 433–460.
Cullen, J. T. (2006), On the nonlinear relationship between dissolved cadmium and phosphate in the modern global ocean: Could chronic iron limitation of phytoplankton growth cause the kink?, *Limnol. oceanogr.*, *51*, 1369–1380.
Cullen, J. T., T. W. Lane, F. M. Morel, and R. M. Sherrell (1999), Modulation of cadmium uptake in phytoplankton by seawater CO_2 concentration, *Nature*, *402*, 165–167.
Delgadillo-Hinojosa, F., J. V. Macıas-Zamora, J. A. Segovia-Zavala, and S. Torres-Valdés (2001), Cadmium enrichment in the Gulf of California, *Mar. Chem.*, *75*(1), 109–122.
Dixon, J. L., P. J. Statham, C. E. Widdicombe, R. M. Jones, S. Barquero-Molina, B. Dickie, M. Nimmo, and C. M. Turley (2006), Cadmium uptake by marine micro-organisms in the English Channel and Celtic Sea, *Aquat. Microbial Ecol.*, *44*(1), 31–43.
Duce, R. A., et al. (1991), The atmospheric input of trace species to the world ocean, *Global Biogeochem. Cycles*, *5*(3), 193–259.
Elderfield, H., and R. Rickaby (2000), Oceanic Cd/P ratio and nutrient utilization in the glacial Southern Ocean, *Nature*, *405*, 305–310.
Finkel, Z. V., A. S. Quigg, R. K. Chiampi, O. E. Schofield, and P. G. Falkowski (2007), Phylogenetic diversity in cadmium: Phosphorus ratio regulation by marine phytoplankton, *Limnol. Oceanogr.*, *52*(3), 1131–1138.
Frew, R. D., and K. A. Hunter (1992), Influence of Southern Ocean waters on the cadmium—phosphate properties of the global ocean, *Nature*, *360*.
Gaudry, A., S. Zeroual, F. Gaie-Levrel, M. Moskura, F. Boujrhal, R. C. Moursli El, A. Guessous, A. Mouradi, T. Givernaud, and R. Delmas (2007), Heavy metals pollution of the Atlantic marine environment by the Moroccan phosphate industry, as observed through their bioaccumulation in Ulva lactuca, *Water Air Soil Pollut.*, *178*, 267–285.
Gault-Ringold, M., T. Adu, C. H. Stirling, R. D. Frew, and K. A. Hunter (2012), Anomalous biogeochemical behavior of cadmium in subantarctic surface waters: Mechanistic constraints from cadmium isotopes, *Earth Planet. Sci. Lett.*, *341*, 94–103.
Gelado-Caballero, M. D., P. López-García, S. Prieto, M. D. Patey, C. Collado, and J. J. Hérnández-Brito (2012), Long-term aerosol measurements in Gran Canaria, Canary Islands: Particle concentration, sources and elemental composition, *J. Geophys. Res.*, *117*, D03304, doi:10.1029/2011JD016646.
Guieu, C., and A. J. Thomas (1996), Saharan aerosols: From the soil to the ocean, in *The Impact of Desert Dust Across the Mediterranean*, pp. 207–216, Springer, Dordrecht, Netherlands.
Guieu, C., M. D. Loÿe-Pilot, L. Benyahya, and A. Dufour (2010), Spatial variability of atmospheric fluxes of metals (Al, Fe, Cd, Zn and Pb) and phosphorus over the whole Mediterranean from a one-year monitoring experiment: Biogeochemical implications, *Mar. Chem.*, *120*(1), 164–178.
Janssen, D. J., T. M. Conway, S. G. John, J. R. Christian, D. I. Kramer, T. F. Pedersen, and J. T. Cullen (2014), Undocumented water column sink for cadmium in open ocean oxygen-deficient zones, Proc. *Natl. Acad. Sci. U. S. A.*, *111*, 6888–6893, doi:10.1073/pnas.1402388111.
Knauer, G., and J. Martin (1981), Phosphorus-cadmium cycling in northeast Pacific waters, *J. Mar. Res.*, *39*, 65–76.
Knoll, M., A. Hernández-Guerra, B. Lenz, F. López Laatzen, F. Machín, T. J. Müller, and G. Siedler (2002), The Eastern Boundary Current system between the Canary Islands and the African Coast, *Deep Sea Res., Part II*, *49*, 3427–3440, doi:10.1016/S0967-0645(02)00105-4.
Kudo, I., H. Kokubun, and K. Matsunaga (1996), Cadmium in the southwest Pacific Ocean two factors significantly affecting the Cd-PO_4 relationship in the ocean, *Mar. Chem.*, *54*(1), 55–67.
Kuss, J., and K. Kremling (1999), Spatial variability of particle associated trace elements in near-surface waters of the North Atlantic (30 N/60 W to 60 N/2 W), derived by large volume sampling, *Mar. Chem.*, *68*, 71–86.
Lachkar, Z., and N. Gruber (2011), What controls biological production in coastal upwelling systems? Insights from a comparative modeling study, *Biogeosciences*, *8*, 2961–2976.
Lam, P. J., J. K. B. Bishop, C. C. Henning, M. A. Marcus, G. A. Waychunas, and I. Y. Fung (2006), Wintertime phytoplankton bloom in the subarctic Pacific supported by continental margin iron, *Global Biogeochem. Cycles*, *20*, GB1006, doi:10.1029/2005GB002557.
Lane, E.S., K. Jang, J. T. Cullen, and M. T. Maldonado (2008), The interaction between inorganic iron and cadmium uptake in the marine diatom Thalassiosira oceanica, *Limnol. Oceanogr.*, *53*, 1784–1789.
Lane, E. S., D. M. Semeniuk, R. F. Strzepek, J. T. Cullen, and M. T. Maldonado (2009), Effects of iron limitation on intracellular cadmium of cultured phytoplankton: Implications for surface dissolved cadmium to phosphate ratios, *Mar. Chem.*, *115*, 155–162.
Lathuilière, C., V. Echevin, and M. Lévy (2008), Seasonal and intraseasonal surface chlorophyll-a variability along the northwest African coast, *J. Geophys. Res.*, *113*, C05007, doi:10.1029/2007JC004433.
Marchesiello, P., J. C. McWilliams, and A. Shchepetkin (2003), Equilibrium structure and dynamics of the California Current System, *J. Phys. Oceanogr.*, *33*, 753–783.
Mittelstaedt, E. (1991), The ocean boundary along the northwest African coast: Circulation and oceanographic properties at the sea surface, *Prog. Oceanogr.*, *26*, 307–355.
Noriki, S., K. Hamahara, and K. Harada (1999), Particulate flux and Cd/P ratio of particulate material in the Pacific Ocean, *J. Oceanogr.*, *55*, 693–703.
Oakley, S. M., P. O. Nelson, and K. J. Williamson (1981), Model of trace-metal partitioning in marine sediments, *Environmental science & technology*, *15*(4), 474–480.
Oudot, C., P. Morin, F. Baurand, M. Wafar, and P. Le Corre (1998), Northern and southern water masses in the equatorial Atlantic: Distribution of nutrients on the WOCE A6 and A7 lines, *Deep Sea Res., Part I*, *45*, 873–902.

Planquette, H., and R. M. Sherrell (2012), Sampling for particulate trace element determination using water sampling bottles: Methodology and comparison to in situ pumps, *Limnol. Oceanogr. Methods*, *10*, 367–388.
Price, N., and F. Morel (1990), Cadmium and cobalt substitution for zinc in a marine diatom, *Nature*, *344*, 658–660.
Prospero, J. M., and T. N. Carlson (1972), Vertical and areal distribution of Saharan dust over the western equatorial North Atlantic Ocean, *J. Geophys. Res.*, *77*(27), 5255–5265.
Quay, P., J. W. Cullen Landing, and P. Morton (2015), Processes controlling the distributions of Cd and PO_4 in the ocean, *Global Biogeochem. Cycles*, *29*, 830–841, doi:10.1002/2014GB004998.
Ras, J., H. Claustre, and J. Huitz (2008), Spatial variability of phytoplankton pigment distributions in the Subtropical South Pacific Ocean: Comparison between in situ and predicted data, *Biogeosciences*, *5*, 353–369.
Riso, R., P. Le Corre, P. Morin, and J.-Y. Cabon (1994), Vertical distribution of cadmium, copper and lead in the eastern Alboran Sea: Enrichment of metals in surface waters, *J. Mar. Syst.*, *5*, 391–399.
Riso, R. D., P. Le Corre, and C. J. Chaumery (1997), Rapid and simultaneous analysis of trace metals (Cu, Pb and Cd) in seawater by potentiometric stripping analysis, *Anal. Chim. Acta*, *351*, 83–89.
Rodríguez, S., J. A. Alastuey, S. Alonso-Pérez, X. Querol, E. Cuevas, J. Abreu-Afonso, M. Viana, N. Pérez, M. Pandolfi, and J. de la Rosa Díaz (2011), Transport of desert dust mixed with North African industrial pollutants in the subtropical Saharan Air Layer, *Atmos. Chem. Phys.*, *11*, 6663–6685.
Saager, P. M., H. J. De Baar, and R. J. Howland (1992), Cd, Zn, Ni and Cu in the Indian Ocean, *Deep Sea Res., Part A*, *39*(1), 9–35.
Schlitzer, R. (2011), Ocean Data View, http://odv.awi.de.
Sherrell, R. M. (1989), The trace metal geochemistry of suspended oceanic particulate matter, Cambridge, Massachusetts Institute of Technology, Ph.D. thesis, 211 pp.
Sunda, W. G., and S. A. Huntsman (2000), Effect of Zn, Mn, and Fe on Cd accumulation in phytoplankton: Implications for oceanic Cd cycling, *Limnol. Oceanogr.*, *45*, 1501–1516.
Tappin, A. D., D. J. Hydes, J. D. Burton, and P. J. Statham (1993), Concentrations, distributions and seasonal variability of dissolved Cd, Co, Cu, Mn, Ni, Pb and Zn in the English Channel, *Cont. Shelf Res.*, *13*(8), 941–969.
Theodosi, C., Z. Markaki, A. Tselepides, and N. Mihalopoulos (2010), The significance of atmospheric inputs of soluble and particulate major and trace metals to the eastern Mediterranean seawater, *Mar. Chem.*, *120*, 154–163.
Tomczak, M. (1981), An analysis of mixing in the frontal zone of South and North Atlantic Central Water off North-West Africa, *Prog. Oceanogr.*, *10*, 173–192.
Twining, B. S., S. Rauschenberg, P. L. Morton, and S. Vogt (2015), Metal contents of phytoplankton and labile particulate material in the North Atlantic Ocean, *Prog. Oceanogr.*, *137*, 261–283.
Van Heukeelem, L., and C. S. Thomas (2001), Computer-assisted high performance liquid chromatography method development with applications to the isolation and analysis of phytoplankton pigments, *J. Chromatogr. A.*, *910*, 31–49.
Vidussi, F., H. Claustre, B. B. Manca, A. Luchetta, and J. C. Marty (2001), Phytoplankton pigment distribution in relation to upper thermocline circulation in the eastern Mediterranean Sea during winter, *J. Geophys. Res.*, *106*(C9), 19,939–19,956.
Waeles, M., J. F. Maguer, F. Baurand, and R. D. Riso (2013), Off Congo waters (Angola Basin, Atlantic Ocean): A hot spot for cadmium-phosphate fractionation, *Limnol. Oceanogr.*, *58*(4), 1481–1490.
Wang, D., T. C. Gouhier, B. A. Menge, and A. R. Ganguly (2015), Intensification and spatial homogenization of coastal upwelling under climate change, *Nature*, *518*, 390–394.
Wilhelmy, S. A. S., and A. R. Flegal (1991), Trace element distributions in coastal waters along the US-Mexican boundary: Relative contributions of natural processes vs. anthropogenic inputs, *Mar. Chem.*, *33*, 371–392.
Wu, J., and S. Roshan (2015), Cadmium in the North Atlantic: Implication for global cadmium-phosphorus relationship, *Deep Sea Research Part II: Topical Studies in Oceanography*, *116*, 226–239.
Xie, R. C., S. J. Galer, W. Abouchami, M. J. Rijkenberg, J. De Jong, H. J. de Baar, and M. O. Andreae (2015), The cadmium-phosphate relationship in the western South Atlantic—The importance of mode and intermediate waters on the global systematics, *Marine Chemistry*, *177*, 110–123.
Xu, Y., L. Feng, P. D. Jeffrey, Y. Shi, and F. M. Morel (2008), Structure and metal exchange in the cadmium carbonic anhydrase of marine diatoms, *Nature*, *452*, 56–61.
Yeats, P. A. (1998), An isopycnal analysis of cadmium distributions in the Atlantic Ocean, *Mar. Chem.*, *61*(1–2), 15–23.
Yeats, P. A., S. Westerlund, and A. R. Flegal (1995), Cadmium, copper and nickel distributions at four stations in the eastern central and south Atlantic, *Mar. Chem.*, *49*(4), 283–293.